

Accepted Manuscript

Title: Performance of Phase-pure M1 MoVNbTeO_x Catalysts by Hydrothermal Synthesis with Different Post-treatments for the Oxidative Dehydrogenation of Ethane

Author: Bozhao Chu Lara Truter T.A. Nijhuis Yi Cheng



PII: S0926-860X(15)00225-2
DOI: <http://dx.doi.org/doi:10.1016/j.apcata.2015.03.039>
Reference: APCATA 15329

To appear in: *Applied Catalysis A: General*

Received date: 30-11-2014
Revised date: 13-3-2015
Accepted date: 26-3-2015

Please cite this article as: B. Chu, L. Truter, T.A. Nijhuis, Y. Cheng, Performance of Phase-pure M1 MoVNbTeO_x Catalysts by Hydrothermal Synthesis with Different Post-treatments for the Oxidative Dehydrogenation of Ethane, *Applied Catalysis A, General* (2015), <http://dx.doi.org/10.1016/j.apcata.2015.03.039>

This is a PDF file of an unedited manuscript that has been accepted for publication. As a service to our customers we are providing this early version of the manuscript. The manuscript will undergo copyediting, typesetting, and review of the resulting proof before it is published in its final form. Please note that during the production process errors may be discovered which could affect the content, and all legal disclaimers that apply to the journal pertain.

Performance of Phase-pure M1 MoVNbTeO_x Catalysts by Hydrothermal Synthesis with Different Post-treatments for the Oxidative Dehydrogenation of Ethane

Bozhao Chu^a, Lara Truter^b, T. A. Nijhuis^{b*}, Yi Cheng^{a*}

^a Department of Chemical Engineering, Beijing Key Laboratory of Green Chemical Reaction Engineering and Technology, Tsinghua University, Beijing 100084, PR China

^b Department of Chemical Engineering and Chemistry, Laboratory of Chemical Reactor Engineering, Eindhoven University of Technology, Eindhoven 5600 MB, The Netherlands

Abstract

Phase-pure M1 catalysts with different post-treatments have been prepared from the same precursor slurry by hydrothermal synthesis and used to study the key factors influencing their performance in the oxidative dehydrogenation of ethane (ODHE) process. Different purification processes (i.e. steam treatment and hydrogen peroxide treatment) result in different tellurium (Te) contents and V⁵⁺ concentration in the catalysts. Catalytic tests reveal that there is a direct correlation between the amount of V⁵⁺ present in the catalysts and the catalytic activity. A hydrogen peroxide treatment increases the V⁵⁺ concentration and decreases the Te content which can improve the catalytic activity and stability in comparison

* **Corresponding Author.** Dr. T.A. Nijhuis, Tel: 31-40-2473671; Fax: 0041-26-3009624;

E-mail address: t.a.nijhuis@tue.nl

* **Corresponding Author.** Dr. Yi Cheng, Tel: 86-10-62794468; Fax: 86-10-62772051;

E-mail address: yicheng@tsinghua.edu.cn

with the steam treatment. A post-treatment with oxalic acid improves the catalyst surface area ($54 \text{ m}^2/\text{g}$) but causes some vanadium leaching. The phase-pure M1 catalyst calcined at $650 \text{ }^\circ\text{C}$ and purified by H_2O_2 shows the best catalyst productivity of $0.77 \text{ kg}_{\text{C}_2\text{H}_4}/\text{kg}_{\text{cat}}/\text{h}$ at 73% ethane conversion and 85% ethylene selectivity in ODHE process. The formation of reduced Te(0) aggregates blocking the active sites is identified as a main reason for catalyst deactivation. A low Te content favors a stable catalyst with less risk of Te aggregation. However, at harsh operating conditions (i.e. high oxygen concentration and high reactor temperature) the performance of phase-pure M1 catalysts with a low Te content can also reduce obviously due to the formation of a new (V, Nb)-substituted $\theta\text{-Mo}_5\text{O}_{14}$ and MoO_2 phases.

Key words: oxidative dehydrogenation, ethane, ethylene, mixed-metal oxide

1. Introduction

Over the years, ethylene has been the largest consumed worldwide chemical commodity due to it being an important building block in the plastics industry. The ethylene production keeps increasing and is expected to reach 150 million tons in 2015 which is 50% more than that in 2005 [1]. Nowadays, ethylene production is mainly based on the petroleum industry. It is mostly produced by steam cracking of various hydrocarbon streams while smaller amounts are obtained by the direct catalytic dehydrogenation of ethane during the fluid-catalytic cracking of gas oils [2]. However, the oxidative dehydrogenation of ethane

(ODHE) has attracted more interest due to the advantages in process performance and energy efficiency [3]. Moreover, ethane, as the only carbon source in the ODHE process, is abundant in main consumer of shale and associated gas. Compared to the limited traditional fossil energy, shale gas has been demonstrated as a new and increasingly important source of natural gas from the start of the 21st century. The global shale gas potential is estimated at about 206.7 trillion cubic meters in 2013 and shale gas development is expected to continue at an accelerated rate around the globe [4]. As a result, abundant ethane with a continuously decreasing price further expands the advantage of the ODHE process.

Catalyst development and research in the ODHE process can be traced back to the 1970's [5]. Some of the catalysts used in the reaction of methane coupling are directly applied in the ODHE process and also some entirely new catalytic systems have been developed during the last 40 years. The catalysts of the ODHE process can be classified based on the active components (i.e. unreducible metal oxides and reducible metal oxides). The unreducible metal oxide catalysts are composed of an alkali metal or alkaline earth metal (i.e. Li, Na, Mg), which is active for both methane coupling and the ODHE process above 600 °C. The reducible metal oxide catalysts consist of transition metals (i.e. Ni, Mo, V), which are active for the oxidative dehydrogenation of alkanes between 300 and 500 °C. The most successful non-reducible catalysts (i.e. Li-O/MgO) can only give a 38% ethane conversion and 80% ethylene selectivity [6] while that of the reducible catalysts (i.e. MoVNbTeO_x) shows a much higher activity and selectivity at a relatively low temperature [7-17]. At 400 °C and 1 atm, the ethane conversion and ethylene selectivity can respectively reach 88.5% and 80.0% with a space time yield of 0.29 kg_{C₂H₄}/kg_{cat}/h [7]. However, the

catalyst performance is still far from the commercial requirement. It has been concluded that the ethane conversion should be in the range of 60-80%, ethylene selectivity higher than 90%, reaction temperature below 500 °C, and productivity of more than 1.00 kg_{C₂H₄}/kg_{cat}/h to realize an economically viable industrial scale production of ethylene based on the ODHE process [18-21].

In the aim of enhancing the catalytic performance (i.e. C₂H₄ conversion, selectivity and productivity), properties of the MoVNbTeO_x catalyst (i.e. chemical and phase composition [7-17], crystal structure [22-27], reaction mechanism and kinetics [28-32]) have been studied in detail.

The MoVNbTeO_x catalyst usually consists of M1 and M2 crystalline phases and minor amounts of other phases such as Mo₅O₁₄-type structures ordinary MoV and MoTe oxides [25]. M1 is an orthorhombic phase with a Pba2 space group. M2 is a pseudo-hexagonal phase with a P6mm space group. The M1 phase is built by center occupied pentagonal rings that are connected by corner sharing MO₆ octahedrons (M = Mo, V), which are assembled in the (001) plane to form characteristic hexagonal and heptagonal rings hosting Te-O units. Only M2 has characteristic hexagonal rings hosting the Te-O units without any pentagonal or heptagonal rings in the (001) plane [24]. It is thought that the M1 phase evolves from the M2 phase by the introduction of Nb⁵⁺ as a pentagonal template leading to the formation of the pentagonal and heptagonal rings [16, 17]. A bronze-like channel structure grows along the (001) direction and a needle-like crystal morphology finally forms in which the (001) planes are perpendicular to the axis length of the needle. It has been demonstrated that terminating (001) planes of the M1 phase cannot supply more activity or selectivity than

other surfaces in the selective oxidation processes [26], however, recently the heptagonal micropores (~ 0.4 nm) of the (001) planes were found to be responsible for the catalytic activity for the ethane selective oxidation [27]. The M1 phase possesses the only V^{5+} and heptagonal channel in the $MoVNbTeO_x$ catalysts [24]. The V^{5+} ions are considered as the active sites for alkane activation [15,24,40]. The M2 phase has more Te^{4+} than the M1 phase, which is considered as the active sites for the activation of α -H in the alkene [24]. As a result, the M2 phase has no activity in the ODHE process and the catalyst performance increases with the M1 phase content in the $MoVNbTeO_x$ catalyst. The phase-pure M1 catalyst is therefore ideal for obtaining a high productivity in the ODHE process.

Commonly, the $MoVNbTeO_x$ catalyst is prepared by either precipitation or hydrothermal synthesis [7-17]. Hydrothermal synthesis is more suitable to prevent the formation of more impure phases than the precipitation method. Although it has been reported that phase-pure M1 catalysts can be directly obtained by hydrothermal synthesis under certain conditions [33], a certain amount of M2 often exists in the catalyst which requires a further post-treatment procedure. According to the different properties of the M1 and M2 phase, some post-treatment methods (i.e. H_2O_2 treatment and steam treatment) are effective in the M1 phase purification [34-36]. However, different post-treatments may not only influence the purity but also the chemical properties and morphology of the catalyst due to its sensitivity to the preparation procedure [37]. Few papers pay attention to the influence of post-treatment on the performance and stability of phase-pure M1 catalyst [38].

In the present work, different post-treatment processes were applied to produce phase-pure M1 catalysts which contain different chemical compositions and surface areas. These four

catalysts were evaluated at different temperatures (340-460 °C) with different feed composition to investigate the effect of different post-treatments on the catalyst performance (ethylene selectivity, productivity and stability) in the ODHE process. All of the catalyst evaluations were carried out in a lab-scale fixed-bed reactor and the properties of the catalyst before and after reaction were characterized by XRD, BET, ICP, XPS, SEM and TEM.

2. Experimental

2.1 Catalyst Preparation

MoVNbTeO_x catalysts were prepared by hydrothermal synthesis [33] and, thereafter, various post-treatment methods were applied.

Ammonium heptamolybdate (Sigma-Aldrich, 99.0%), vanadyl sulfate (Sigma-Aldrich, 97%), telluric acid (Sigma-Aldrich, 98%) and ammonium niobium oxalate (Sigma-Aldrich, 99.99%) were used as starting materials to prepare the initial precursor slurry with a molar ratio of 1 Mo:0.25 V:0.12 Nb:0.23 Te. After preparation of the precursor slurry, the slurry was inserted into 100ml Teflon-lined autoclaves and the residual air was replaced by nitrogen. Hydrothermal synthesis was carried out at 175 °C for 48 h. The resulting powder was filtered and washed thoroughly with distilled water, followed by drying for 16 h at 80 °C in air, and calcination for 2 h at 600 °C. The MoVNbTeO_x catalyst was further purified by removal of the M2 phase to form the phase-pure M1 catalyst using various post-treatment procedures. Catalyst A was purified during the calcination step where steam was introduced into the tube-oven to accelerate the decomposition of the M2 phase under hydrothermal synthesis conditions. Catalyst B was obtained by the dissolution of the M2

phase in a 7.5% H₂O₂ solution at 60 °C for 3 h, followed by filtration, washing and drying overnight at 110 °C [35]. Other post-treatment methods were also used to generate phase-pure M1 catalyst with different morphology and chemical composition. Catalyst C was obtained by calcination at 650 °C for 2 h, followed by the purification in a 7.5% H₂O₂ solution as described previously. Catalyst D was obtained after an initial oxalic acid post-treatment followed by calcination 600 °C for 2 h and the 7.5% H₂O₂ purification steps. The oxalic acid post-treatment was carried out in 60 mmol/ml oxalic acid solution at 60 °C for 2 h for the catalyst only after hydrothermal synthesis, filtration, washing and drying. The oxalic acid treatment was originally used in the purification of orthorhombic Mo₃VO_x oxides [27].

2.2 Catalyst Testing

The M1 catalysts were prepared for catalytic testing by diluting with SiC powder in a 1:4 ratio to improve the heat distribution during the reaction and, thereafter, pelletized to a 100 – 200 µm particle size. 0.625 g catalyst was loaded in a quartz tube (6 mm i.d. and 750 mm length) and operated isothermally at atmospheric pressure. The gas feed consisted of ethane, oxygen and helium with the total flow rate of 30 Nml/min and a C₂H₆/O₂/He molar ratio of 30/20/50. The space time $W/F_{C_2H_6}$ (W is the catalyst mass and $F_{C_2H_6}$ is the ethane molar flow rate) was maintained at 20.74 g_{cat}·h/mol_{C₂H₆} and the reaction temperature varied between 360 and 460 °C. During the heating up of the fixed-bed reactor, helium is the only gas fed through the reactor tube. Once the reaction temperature was reached, the reagent and the gas feed with the appropriate composition were introduced into the system. The steady-state data of catalyst performance was determined 6h after the beginning of the reaction because

there is usually an induction period for the catalysts in oxidative dehydrogenation of alkanes.

The reactor effluent was analyzed by an online gas chromatography (GC) equipped with two columns. A PorapakQ column was used to separate the CO₂, C₂H₄ and C₂H₆ and 5A molecular sieve column was used to separate the O₂, N₂, CH₄ and CO. A blank run was conducted by loading the reactor with only SiC and using the same operating conditions. No ethane conversion was observed indicating that the effect of the homogeneous gas phase reaction can be neglected.

The conversion and selectivity for ODHE process are defined as follows:

$$X_{C_2H_6} = \left(1 - \frac{2f_{C_2H_6}}{2f_{C_2H_6} + 2f_{C_2H_4} + f_{CO} + f_{CO_2}} \right) \times 100\% \quad (1)$$

$$S_{C_2H_4} = \left(\frac{2f_{C_2H_4}}{2f_{C_2H_4} + f_{CO} + f_{CO_2}} \right) \times 100\% \quad (2)$$

$$S_{CO_2} = \left(\frac{f_{CO_2}}{2f_{C_2H_4} + f_{CO} + f_{CO_2}} \right) \times 100\% \quad (3)$$

$$S_{CO} = \left(\frac{f_{CO}}{2f_{C_2H_4} + f_{CO} + f_{CO_2}} \right) \times 100\% \quad (4)$$

Where, X is the ethane conversion, S is the selectivity to a certain product, and f is the molar fraction in the effluent gas.

2.3 Catalyst Characterization

X-ray diffraction (XRD) patterns of samples were recorded on a Bruker D8 Advance equipment with Cu K α radiation in the 2θ range of 5-50°. Phase identification of the catalysts was carried out by comparing the collected spectra with those listed in the JCPDS

database (Joint Committee of Powder Diffraction Standards) and the ICSD database (Inorganic Crystal Structure Database). According to the ICSD database, M1 phase (ICSD 55097) has characteristic diffraction lines located at $2\theta = 6.6, 7.7, 8.9, 22.1, \text{ and } 27.1^\circ$ and the M2 phase (ICSD 55098) at $2\theta = 22.1, 28.1 \text{ and } 36.2^\circ$. The average particle diameter along a certain direction was calculated with the Scherrer equation.

The specific surface area was calculated based on the multipoint Brunauer–Emmett–Teller method (BET) in the $p/p_0 = 0.05\text{-}0.30$ pressure range. Nitrogen adsorption was carried out at 77 K on a Quantachrome Autosorb-6B analyzer. Prior to the measurement, the samples were degassed in vacuum at 110°C for 2 h. Inductively coupled plasma-optical emission spectrometry (ICP-OES, Varian Vista RL spectrometer) was used to analyze the metal content of the MoVNbTeO_x catalyst.

The morphology and particle size distribution was characterized using a scanning electron microscopy (SEM, JEOL, JSM-7401F) and a JEOL JEM2010 high-resolution transmission electron microscopy (HR-TEM). TEM samples were prepared by dispersing 0.01 g catalyst powder in 5ml ethanol by ultrasonic agitation. Thereafter, the suspension was dropped onto a carbon-coated copper grid and dried in air at 110°C for 2 h.

X-ray photoelectron spectra (XPS) was acquired using a PHI Quantera SXM system, equipped with Al $K\alpha$ X-ray source. The binding energy data of reference material is obtained from NIST X-ray Photoelectron Spectroscopy Database. Survey scans (0-1200 eV) and high-resolution Mo (3d), V (2p), Te (3d), Nb (3d) and C (1s) spectra were obtained. To obtain accurate results of valance distribution by de-convolution, the dwell time was increased from 300 ms to 500 ms and the scan times were increased from 6 to 10 during the

high-resolution scanning for V and Te. The uncertainty of the peak positions was estimated to be 0.2 eV for all spectra and the binding energy (BE) scale was calibrated by setting the C (1s) transition to 284.8 eV. The analysis of the measured high-resolution spectra was performed using XPSPEAK 4.1 software.

The hydrogen peroxide concentration was verified by a hydrogen peroxide titration with a standard solution of cerium (IV) sulfate.

3. Results and Discussion

3.1 General Properties of MoVNbTeO_x Catalysts

The chemical and structural details of the MoVNbTeO_x catalysts are summarized in Table 1 and the XRD patterns of the respective catalysts are presented in Figure 1.

[Table 1]

[Figure 1]

Without applying a purification treatment, the hydrothermally synthesized, Catalyst E, contains small amounts (~20 wt %) of the M2 phase. The removal of the M2 phase was made possible by applying either a steam treatment (Catalyst A) or a H₂O₂ treatment (Catalyst B, C& D) which resulted in the phase-pure M1 catalysts.

However, despite these catalysts all containing only the M1 phase, the different post-treatment processes were seen to greatly influence the final chemical composition of the MoVNbTeO_x catalysts (despite being prepared from the same precursor slurry). Catalyst A, which was calcined in the presence of steam, produced the M1 phase catalyst with a high

tellurium content. The presence of the steam was thought to inhibit the volatilization of tellurium during the calcination step. However, despite the higher amount of Te in Catalyst A, no Te metal is seen in the XRD patterns or XPS measurements (Figure 2 & 3). Previously, it has been shown that a steam post-treatment enables the formation of phase-pure M1 but with the additional formation of metallic Te [35]. However, this was not observed which could be due to the milder post-treatment conditions. Meanwhile, the post-treatment with oxalic acid resulted in the vanadium content of Catalyst D to be lower. This loss in vanadium could be caused from the vanadium being leached from the M1 crystalline structure due to it being more soluble in comparison to other elements. In addition, the crystal structure of all the catalyst was comparable with the pure M1 phase [39].

The morphology of catalysts also indicated obvious differences after the various treatments. TEM and SEM images of the respective catalysts are shown in Figure 2.

[Figure 2]

The particle size and surface area of the catalysts were seen to decrease in the following order: Catalyst A > B > C > D. Catalyst D, prepared from the oxalic acid post-treatment resulted in the largest decrease in particle size to approximately 22 nm. The surface area was approximately 54 m²/g which is the largest among the MoVNbTeO_x catalysts reported in literature. It is thought that the precursor material of long-range ordering in the [001] direction formed during the hydrothermal synthesis [33] are tapered by oxalic acid resulting in the formation of smaller needle-like crystals. Catalyst C which was calcined at a higher temperature (650 °C) was found to give a smaller particle size and larger surface area in comparison to Catalyst B (calcined at 600 °C).

3.2 XPS Analysis

Figure 3 shows XPS spectra of the key elements in the MoVNbTeO_x catalysts which were measured to investigate the element valence state on the catalyst surface.

[Figure 3]

For all catalysts, the binding energy (BE) of molybdenum (232.8 eV) and niobium (207.2 eV) corresponds well to the typically reported binding energies for MoO₃ and Nb₂O₅ which suggests a single molybdenum and niobium valence state of +6 and +5, respectively. Tellurium has a binding energy between 576.5±0.1 eV for TeO₂ and 577.3±0.1 eV for TeO₃ which implies the presence of both the Te⁴⁺ and Te⁶⁺ species. The molar ratio of Te⁶⁺ and Te⁴⁺ maintains the similar value between 0.49 and 0.53 by the de-convolution of the Te 3d_{5/2} core level spectra [40]. No formation of Te⁰ (573.2±0.1 eV) was detected. It indicates that the valences distribution of Te on the surface of catalysts almost make no difference to the catalyst performance.

The binding energy of vanadium is between the value of 516.3±0.1 eV for VO₂ and 517.2±0.1 eV for V₂O₅, inferring that vanadium has two valence states of +4 and +5 [40]. Since V⁵⁺ is considered the only active site for ethane activity, the abundance of these V⁵⁺ species remains an important factor affecting the catalyst performance (Section 3.3). The abundance of the V⁵⁺ species on the respective catalyst surfaces was calculated by combination of the elemental composition and de-convolution of the vanadium 2p_{3/2} peak (Figure 3).

Catalysts B, C and D show a higher percentage of V⁵⁺ content in comparison to Catalyst A

which could be attributed to the H₂O₂ treatment where the oxidative property of the H₂O₂ may favor the formation of V⁵⁺ from V⁴⁺. Catalyst D shows the lowest quantity of total vanadium due to the leaching of vanadium during the oxalic acid post-treatment step. However, a high portion of the vanadium is in the V⁵⁺ valance state which, similarly, can be attributed to the H₂O₂ treatment. The effect of the V⁵⁺ quantity on the catalytic activity of the respective catalysts is further discussed in section 3.3.

3.3 Catalytic Evaluation of MoVNbTeO_x Catalysts

Figure 4 shows the catalytic performance of the respective catalysts in the ODHE process.

[Figure 4]

The catalytic performance of the respective catalysts shows great variations in productivity depending on the post-treatment method used. Catalyst B and Catalyst C show good performance at 400 °C with ethane conversions of 74.2% and 76.9%. This is consistent with Catalysts B and C having the highest V⁵⁺ concentration. Catalyst D has a catalytic activity which follows the same trend of the V⁵⁺ concentration in the respective catalysts. Although, the total V content was lower for Catalyst A, the higher V⁵⁺ content still ensured a greater catalytic activity. The smaller particle size and larger surface area of Catalyst D is seen to not affect the catalytic performance significantly where Catalyst B and C with larger particle size and smaller surface area have a higher activity. It was similarly found by *Kolen'ko et al.* [36] that the particle size and surface area do not influence the catalytic performance for the selective oxidation of propane. Catalyst A shows the lowest productivity due to the low ethane conversion which can be attributed to the low V⁵⁺ abundance. Since the surface

oxidation state of vanadium varies in the reaction conditions and a re-equilibration takes place under reaction conditions[40], the V^{5+} abundance of the catalysts after a 6 h catalytic test was also measured as illustrated in Figure S1. Although the total vanadium and V^{5+} abundance was slightly higher after the reaction, the sequence of the catalyst based on the V^{5+} abundance did not change. Moreover, the high Te content could also affect the activity by increasing the occupancy of Te-O unit located in the heptagonal channel of M1 phase which has been recently demonstrated by *Ishikawa et al.* [27] as the necessary path way for ethane to be selectively oxidized to ethylene.

It can therefore be concluded that the V^{5+} concentration, not the total amount of V [10], is the main factor affecting the catalytic activity of the catalyst where the catalyst morphology, particle size and surface area do not significantly affect the catalytic activity. It is thought that the H_2O_2 treatment is important in the oxidation of the $MoVNbTeO_x$ catalyst due to its ability to increase the V^{5+} content. Since the V content of Catalyst A, B and C is similar and all are phase-pure M1, the higher V^{5+} content can be ascribed to the H_2O_2 increasing the formation of V^{5+} from V^{4+} sites. The extent of the M2 removal during the H_2O_2 treatment could also affect the V^{5+} concentration since V^{5+} is not present in the M2 phase [34]. However, as seen in the XRD patterns (Figure 2), the respective catalysts are all pure M1 phase and contain similar quantities of total V, so the differences in V^{5+} concentration is thought to be due to the oxidative properties of the H_2O_2 .

To further investigate this, the H_2O_2 concentration was varied (2.5 - 10%) and the effect on the V^{5+} abundance in the catalyst and catalytic activity was determined (Figure 5).

[Figure 5]

As the H_2O_2 concentration increases, the V^{5+} concentration increases together with the ethane conversion. This indicates that the H_2O_2 treatment step is an effective method for increasing the V^{5+} concentration in the catalyst. All the catalysts used in this experiment have been demonstrated as phase-pure M1 by XRD and similar Te content by ICP. So it is sufficient to remove the M2 phase and decrease Te content even by using the H_2O_2 solution with the concentration as low as 2.5%.

The ethylene selectivity determines the atom economy of the ODHE process. The selectivity of propane selective oxidation on MoVNbTeO_x catalyst has been discussed extensively in literature but few focus on the selectivity of the ODHE process [41-46]. In this work, at the same ethane conversion level of approximately 45%, Catalyst A, B and C show a similar ethylene selectivity of 85% whilst Catalyst D gives a lower ethylene selectivity of 80%. As proposed by *Grasselli* [44], the deep oxidation of ethane and ethylene to CO_x on MoVNbTeO_x catalysts can be suppressed by spatially isolating the active sites. According to *Ueda et al.*[45-46], the Nb species can promote rapid desorption of the desired products so as to prevent further oxidation and increase the selectivity. But this theory cannot be used to explain the low selectivity of Catalyst D since there is no obvious loss of Nb during the oxalic acid treatment based on the XPS and ICP chemical composition analyses. It is deduced that oxalic acid treatment may destroy the crystal structure of the M1 phase which affects the ethylene selectivity. The oxalic acid treatment could therefore provide an opportunity to detect the key factors of the M1 phase's crystal structure in the selectivity of the ODHE process.

3.4 Stability of Phase-pure M1 Catalysts

In addition to the activity and selectivity, the stability of the catalyst is also a significant factor in the realization of an industrial-scale production process. Time-on-stream and harsh operating conditions (i.e. high temperature and high oxygen concentration) experiments of the respective catalysts were performed in order to investigate the stability and main deactivation factors of the phase-pure M1 catalyst.

3.4.1 Stability of Phase-pure M1 Catalysts with Different Te Content

The time-on-stream as a function of ethane conversion and ethylene selectivity at standard operating conditions is shown in Figure 6 for Catalyst A (high Te content) and Catalyst B (low Te content). Catalyst C and D show similar Te content and stability in comparison to Catalyst B and are thus not included. Different flow rates of feed gas are used to keep Catalyst A and B at similar ethane conversion levels at the start of the experiment in order to compare the stability.

[Figure 6]

Over a 36 h time-on-stream period, Catalyst A is seen to deactivate from 32% to 28% ethane conversion whilst Catalyst B remains stable at 31%. The reason for this difference in deactivation can be provided by XRD and XPS measurements of the used catalyst (Figure 7).

[Figure 7]

XRD results demonstrate that Te exists in the used Catalyst A while XPS results similarly indicate that Te^0 is produced by the reduction of Te^{4+} . Moreover, ICP chemical analysis

indicates that the Te content of Catalyst A does not significantly change after the reaction. It is therefore thought that Te is reduced from Te^{4+} to form Te^0 on the catalyst surface which blocks the active sites or heptagonal channels resulting in the higher rate of deactivation with time for Catalyst A, containing a higher Te content. This conclusion is consistent with the research of *Valente et al.* [38] in the ODHE process over the MoVNbTeO_x catalyst composed of both the M1 phase and M2 phase. For Catalyst B, containing a lower Te content, there is no detectable formation of metallic Te from the XRD and XPS results. The avoidance of the formation of metallic Te is thus important for obtaining a highly stable catalyst. Catalyst preparation should keep Te content at moderate levels.

3.4.2 Stability of Phase-pure M1 Catalysts with low Te content under harsh condition

The stability of Catalyst B, with a low Te content, was evaluated at harsh operating conditions of high oxygen concentration in the feed stream (Figure 8A) and high reactor operating temperature (Figure 8B).

[Figure 8]

After a 24h time-on-stream period there is a 45% deactivation for the higher oxygen concentration feed conditions and a 10% deactivation for the catalyst operating at a high reactor temperature. XRD analyses of the fresh and used Catalyst B are shown in Figure 10. At high oxygen concentration conditions, a (V, Nb)-substituted $\theta\text{-Mo}_5\text{O}_{14}$ (JCPDS 31-1437) phase forms in addition to the M1 phase. Whereas, at high reactor temperature conditions, a MoO_2 (JCPDS 32-0671) forms. The (V, Nb)-substituted $\theta\text{-Mo}_5\text{O}_{14}$ phase has little activity in the ODHE process whilst the MoO_2 phase has no activity in the ODHE reaction [10]. It is

verified by ICP analysis that there is approximately 25% weight loss of Te in Catalyst B after the reaction under high temperature conditions. The formation of these new phases with less or no ODHE activity by the loss of Te under harsh conditions is thus the main reason for the deactivation. The leaching of Te was also observed in MoVNbTeO_x catalyst containing both M1 and M2 phases [38]. The precise control of oxygen concentration and reactor temperature is a prerequisite to maintain a high stability and phase-pure M1 catalyst in the ODHE process.

[Figure 9]

4. Conclusion

The influence of post-treatment steps in the preparation of phase-pure M1 MoVNbTeO_x catalysts has been studied in this work. Excellent catalytic performance in the ODHE process with ethane conversion of 73%, ethylene selectivity of 85% and space-time yield of 0.77 kg_{C₂H₄}/kg_{cat}/h was obtained by a combination of high calcination temperature (650 °C) and H₂O₂ treatment. The V⁵⁺ concentration was found to be the main factor influencing the phase-pure M1 catalyst activity and its stability was dependent on the Te content. Besides the function of purification for M1 phase, H₂O₂ treatment was demonstrated as an effective method to increase the V⁵⁺ abundance on the catalyst surface and decrease the Te content in the catalyst bulk which can improve the phase-pure M1 catalyst activity and stability in ODHE process. Other post-treatment procedures, such as treatment with oxalic acid, resulted in a significantly lower particle size (23 nm) and higher surface area (54 m²/g). However, loss of vanadium during this treatment reduced its catalytic activity despite the

improvements in surface morphology. Moreover, harsh operating conditions such as high oxygen concentration in the feed gas and high reactor operating temperature can also result in the deactivation even in catalysts with low Te content. It is, therefore, recommended that catalysts with high vanadium content and moderate Te content be synthesized and operated in the ODHE process at moderate oxygen feed concentrations and reactor temperatures (< 460 °C).

Acknowledgements

Financial supports from joint project supported by KNAW and Ministry of Education (China) are acknowledged.

References

- [1] W.R. True, *Oil. Gas. J.* 110(2012) 78-84.
- [2] M.A. Banares, *Catal. Today.* 51 (1999) 319-348.
- [3] C.A. Gärtner, A.C. van Veen, J.A. Lercher, *ChemCatChem.* 5 (2013) 3196-3217.
- [4] M. Melikoglu, *Renew. Sus. Energ. Rev.* 37 (2014) 460-468.
- [5] E.M. Thorsteinyon, T.P. Wilson, F.G. Young, *J. Catal.* 116-132 (1978).
- [6] F. Cavani, *Catal. Today.* 24 (1995) 307-313.
- [7] J.M. López Nieto, P. Botella, M.I. Vázquez, A. Dejoz, *Chem. Commun.* (2002) 1906-1907.
- [8] P. Botella, J.M. López Nieto, A. Dejoz, M.I. Vázquez, A. Martínez-Arias, *Catal. Today.* 78 (2003) 507-512.

- [9] J.M. López Nieto, P. Botella, P. Concepción, A. Dejoz, M.I. Vázquez, *Catal. Today*. 91-92 (2004) 241-245.
- [10] P. Botella, E. García-González, A. Dejoz, J.M. López Nieto, M.I. Vázquez, J. González-Calbet, *J. Catal.* 225 (2004) 428-438.
- [11] Q. Xie, L. Chen, W. Weng, H. Wan, *J. Mole. Catal. A-Chem.* 240 (2005) 191-196.
- [12] B. Solsona, M. Vazquez, F. Ivars, A. Dejoz, P. Concepcion, J.M. Lopez Nieto, *J. Catal.* 252 (2007) 271-280.
- [13] T.T. Nguyen, M. Aouine, J.M.M. Millet, *Catal. Commun.* 21 (2012) 22-26.
- [14] T.T. Nguyen, L. Burel, D.L. Nguyen, C. Pham-Huu, J.M.M. Millet, *Appl. Catal. A- Gen.* 433-434 (2012) 41-48.
- [15] T.T. Nguyen, B. Deniau, P. Delichere, J.M. Millet, *Top. Catal.* 57 (2014) 1152-1162.
- [16] M. Baca, A. Pigamo, J.L. Dubois, J.M.M. Millet, *Catal. Commun.* 6 (2005) 215-220.
- [17] P. Concepción, S. Hernández, J.M. López Nieto, *Appl. Catal. A- Gen.* 391 (2011) 92-101.
- [18] M.M. Bhasin, *Top. Catal.* 23 (2003) 145-149.
- [19] D. Sanfilippo, I. Miracca, *Catal. Today*. 111 (2006) 133-139.
- [20] F. Cavani, N. Ballarini, A. Cericola, *Catal. Today*. 127 (2007) 113-131.
- [21] G. Grubert, E. Kondratenko, S. Kolf, M. Baerns, P. van Geem, R. Parton, *Catal. Today*. 81 (2003) 337-345.
- [22] F. Cavani, N. Ballarini, A. Cericola, *Catal. Today*. 127 (2007) 113-131.
- [23] J.M. López Nieto, P. Botella, B. Solsona, J.M. Oliver, *Catal. Today*. 81 (2003) 87-94.
- [24] R.K. Grasselli, D.J. Buttrey, P. DeSanto, J.D. Burrington, C.G. Lugmair, A.F. Volpe, T.

- Weingand, *Catal. Today*. 91-92 (2004) 251-258.
- [25] M. Aouine, J.M.M. Millet, J.L. Dubois, *Chem. Commun.* (2001) 1180-1181.
- [26] A. Celaya Sanfiz, T.W. Hansen, A. Sakthivel, A. Trunschke, R. Schlögl, A. Knoester, H.H. Brongersma, M.H. Looi, S.B.A. Hamid, *J. Catal.* 258 (2008) 35-43.
- [27] S. Ishikawa, X. Yi, T. Murayama, W. Ueda, *Appl. Catal. A- Gen.* 474 (2014) 10-17.
- [28] M.D. Argyle, K. Chen, A.T. Bell, E. Iglesia, *J. Phys. Chem. B.* 106 (2002) 5421-5427.
- [29] F. Klose, *Appl. Catal. A- Gen.* 260 (2004) 101-110.
- [30] C.A. Gärtner, A.C. van Veen, J.A. Lercher, *ChemCatChem.* 5 (2013) 3196-3217.
- [31] G. Che-Galicia, R. Quintana-Solórzano, R.S. Ruiz-Martínez, J.S. Valente, C.O. Castillo-Araiza, *Chem. Eng. J.* 252 (2014) 75-88.
- [32] J.S. Valente, R. Quintana-Solórzano, H. Armendáriz-Herrera, G. Barragán-Rodríguez, J.M. López-Nieto, *Ind. Eng. Chem. Res.* 53 (2014) 1775-1786.
- [33] A. Celaya Sanfiz, T.W. Hansen, F. Girgsdies, O. Timpe, E. Rödel, T. Ressler, A. Trunschke, R. Schlögl, *Top. Catal.* 50 (2008) 19-32.
- [34] M. Baca, M. Aouine, J.L. Dubois, J.M.M. Millet, *J. Catal.* 233 (2005) 234-241.
- [35] B. Deniau, G. Bergeret, B. Jouguet, J.L. Dubois, J.M.M. Millet, *Top. Catal.* 50 (2008) 33-42.
- [36] Y.V. Kolen'Ko, W. Zhang, R.N. D'Alnoncourt, F. Girgsdies, T.W. Hansen, T. Wolfram, R. Schlögl, A. Trunschke, *ChemCatChem.* 3 (2011) 1597-1606.
- [37] X. Yang, R. Feng, W. Ji, C. Au, *J. Catal.* 253 (2008) 57-65.
- [38] J.S. Valente, H. Armendáriz-Herrera, R. Quintana-Solórzano, P. Del Ángel, N. Nava, A. Massó, J.M. López Nieto, *ACS Catal.* 4 (2014) 1292-1301.

- [39]P. DeSanto Jr, D.J. Buttrey, R.K. Grasselli, C.G. Lugmair, A.F. Volpe, B.H. Toby, T. Vogt, *Top. Catal.* 23 (2003) 23-38.
- [40]M. Hävecker, S. Wrabetz, J. Kröhnert, L. Csepei, R. Naumann D Alnoncourt, Y.V. Kolen Ko, F. Girgsdies, R. Schlögl, A. Trunschke, *J. Catal.* 285 (2012) 48-60.
- [41]R.K. Grasselli, J.D. Burrington, D.J. Buttrey, P. DeSanto Jr., C.G. Lugmair, A.F. Volpe Jr., T. Weingand, *Top. Catal.* 23 (2003) 5-22.
- [42]P. Botella, B. Solsona, A. Martinez-Arias, J.M. López Nieto, *Catal. Lett.* 74 (2001) 149-154.
- [43]F.N. Naraschewski, C. Praveen Kumar, A. Jentys, J.A. Lercher, *Appl. Catal. A- Gen.* 391 (2011) 63-69.
- [44]R.K. Grasselli, *Catal. Today.* 99 (2005) 23-31.
- [45]W. Ueda, D. Vitry, T. Katou, *Catal. Today.* 99 (2005) 43-49.
- [46]W. Ueda, D. Vitry, T. Katou, *Catal. Today.* 96 (2004) 235-240.

Figures Captions

Figure 1 XRD patterns (above) and enlargement of region from $2\theta = 26-30^\circ$ (below) of the MoVNbTeO_x catalysts. (A) Catalyst A; (B) Catalyst B; (C) Catalyst C; (D) Catalyst D (E) Catalyst without post-treatment

Figure 2 TEM and SEM images of the fresh MoVNbTeO_x catalysts

Figure 3 XPS spectra of the (A) Catalyst A, (B) Catalyst B, (C) Catalyst C and (D) Catalyst D for the main transition elements and V⁵⁺ abundance in fresh catalyst A-D

Figure 4 MoVNbTeO_x catalyst performance in the ODHE process as a function of reaction temperature for (A) ethane conversion, (B) oxygen conversion, (C) ethylene selectivity, (D) CO selectivity and (E) CO₂ selectivity, at space time of 20.74 g_{cat}·h/mol_{C₂H₆} and feed molar ratio of C₂H₆/O₂/He = 30/20/50.

Figure 5 Ethane conversion and V⁵⁺/V⁴⁺ molar ratio as a function of H₂O₂ concentration during post-treatment for catalyst B. Catalytic experiments were performed at 420 °C with a space time of 20.74 g_{cat}·h/mol_{C₂H₆} and a reactor inlet C₂H₆/O₂/He molar ratio of 30/20/50

Figure 6 Ethane conversion and ethylene selectivity as functions of time-on-stream for catalyst A and B. Experiments were performed at 420 °C with a space time of 20.74 g_{cat}·h/mol_{C₂H₆} for Catalyst A and 6.91 g_{cat}·h/mol_{C₂H₆} for Catalyst B and a reactor inlet C₂H₆/O₂/He molar ratio of 30/20/50

(■) ethane conversion of catalyst A (□) ethylene selectivity of Catalyst A

(●) ethane conversion of catalyst B (○) ethylene selectivity of Catalyst B

Figure 7 XRD patterns (above) and XPS spectra (below) for used catalyst (A) Catalyst A and (B) Catalyst B

Figure 8 Ethane conversion (●) and ethylene selectivity (○) as functions of time-on-stream for catalyst B under harsh conditions. Experiments were performed at (A) 420 °C with a space time of 20.74 g_{cat}·h/mol_{C₂H₆} and a reactor inlet C₂H₆/O₂/He molar ratio of 30/40/30 and (B) 460 °C with a space time of 20.74 g_{cat}·h/mol_{C₂H₆} and a reactor inlet C₂H₆/O₂/He molar ratio of 30/20/50

Figure 9 XRD patterns of (A) fresh catalyst B (B) used catalyst B after ODHE in high O₂ concentration and (C) used catalyst B after ODHE at high temperature

Table Captions**Table 1** General properties of the MoVNbTeO_x catalysts

Accepted Manuscript

Figures

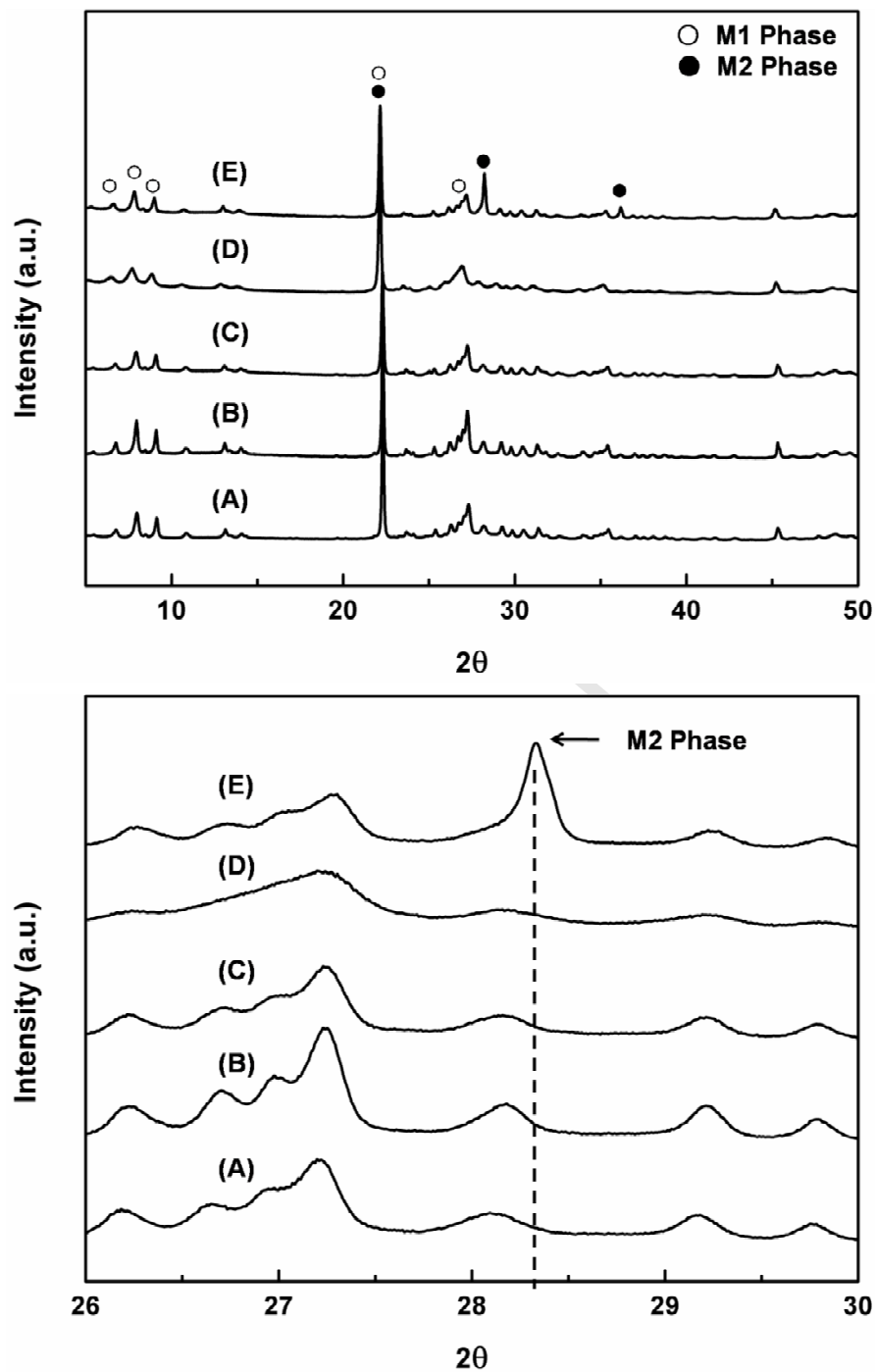


Figure 1 XRD patterns (above) and enlargement of region from $2\theta = 26$ - 30° (below) of the MoVNbTeO_x catalysts. (A) Catalyst A; (B) Catalyst B; (C) Catalyst C; (D) Catalyst D (E) Catalyst without post-treatment

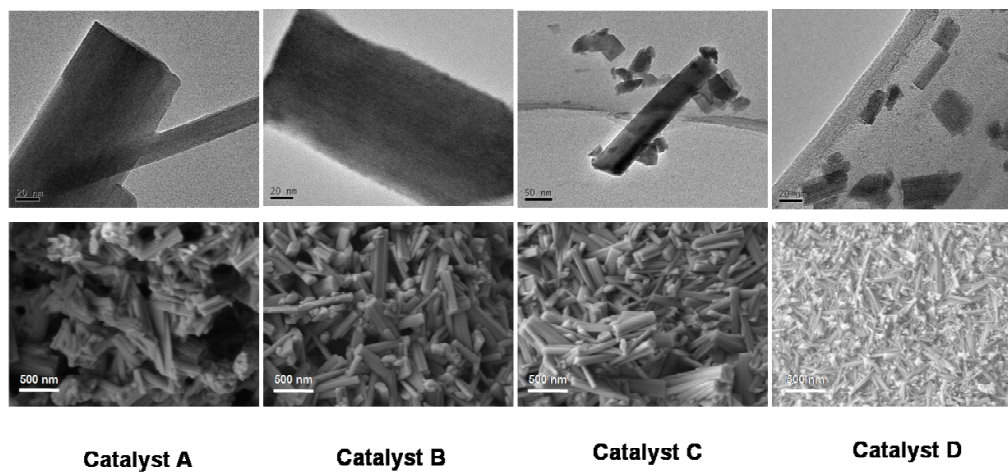


Figure 2 TEM and SEM images of the fresh MoVNbTeO_x catalysts

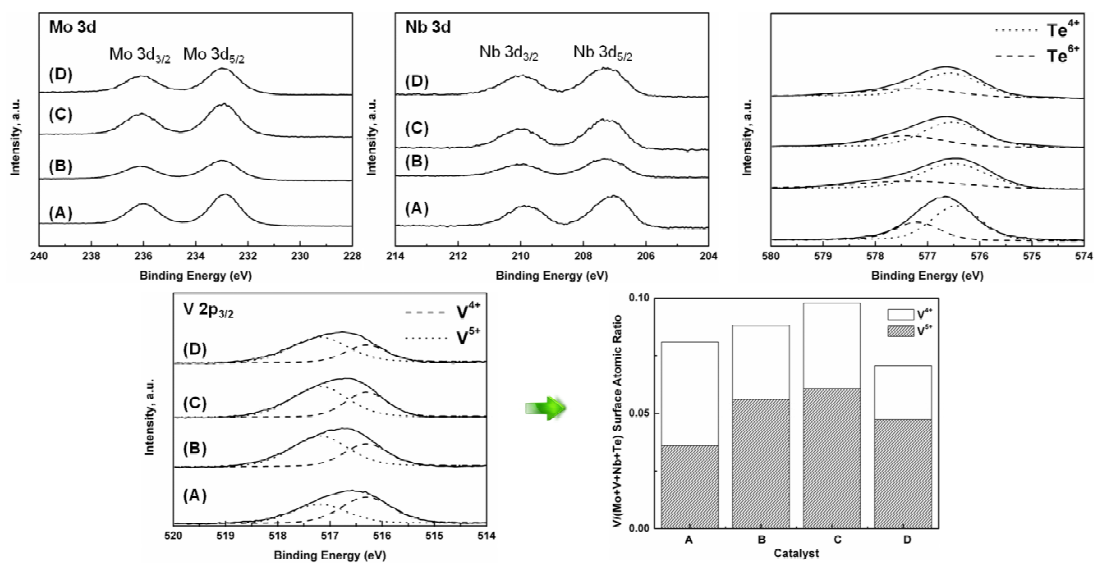


Figure 3 XPS spectra of the (A) Catalyst A, (B) Catalyst B, (C) Catalyst C and (D) Catalyst D for the main transition elements and V⁵⁺ abundance in fresh catalyst A-D

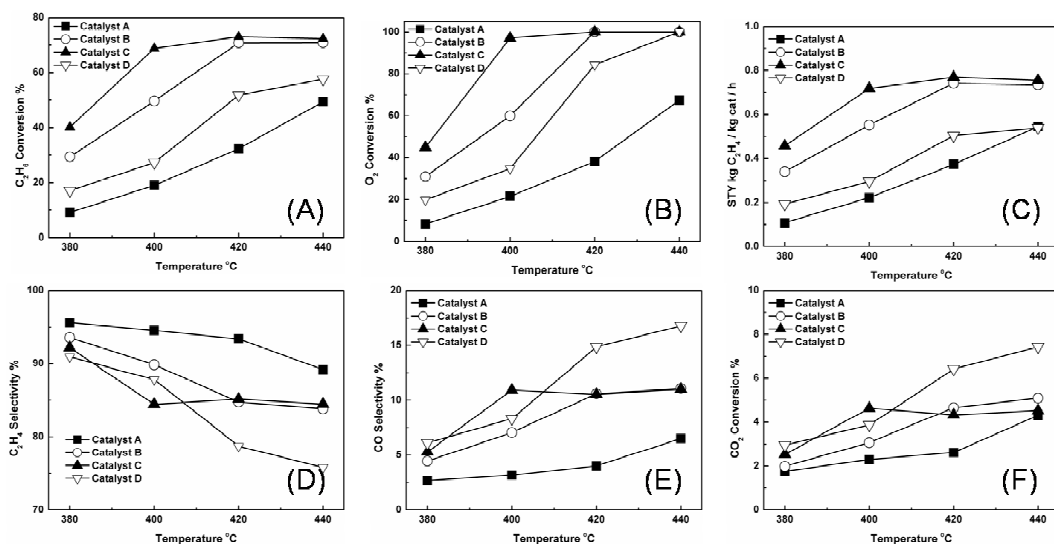


Figure 4 MoVNbTeO_x catalyst performance in the ODHE process as a function of reaction temperature for (A) ethane conversion, (B) oxygen conversion, (C) ethylene space-time yield (D) ethylene selectivity, (E) CO selectivity and (F) CO₂ selectivity, at space time of 20.74 g_{cat}·h/mol_{C₂H₆} and feed molar ratio of C₂H₆/O₂/He = 30/20/50.

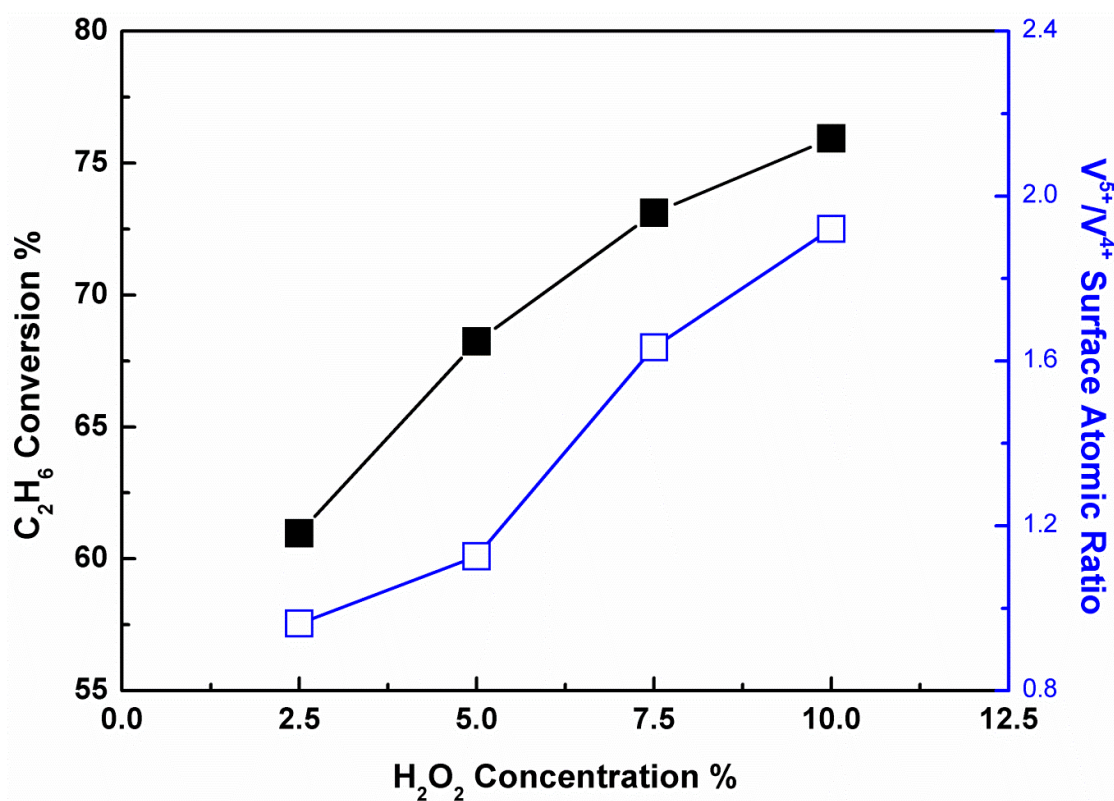


Figure 5 Ethane conversion and V⁵⁺/V⁴⁺ surface atomic ratio as a function of H₂O₂ concentration during post-treatment for catalyst B. Catalytic experiments were performed at 420 °C with a space time of 20.74 g_{cat}·h/mol_{C₂H₆} and a reactor inlet C₂H₆/O₂/He molar ratio of 30/20/50.

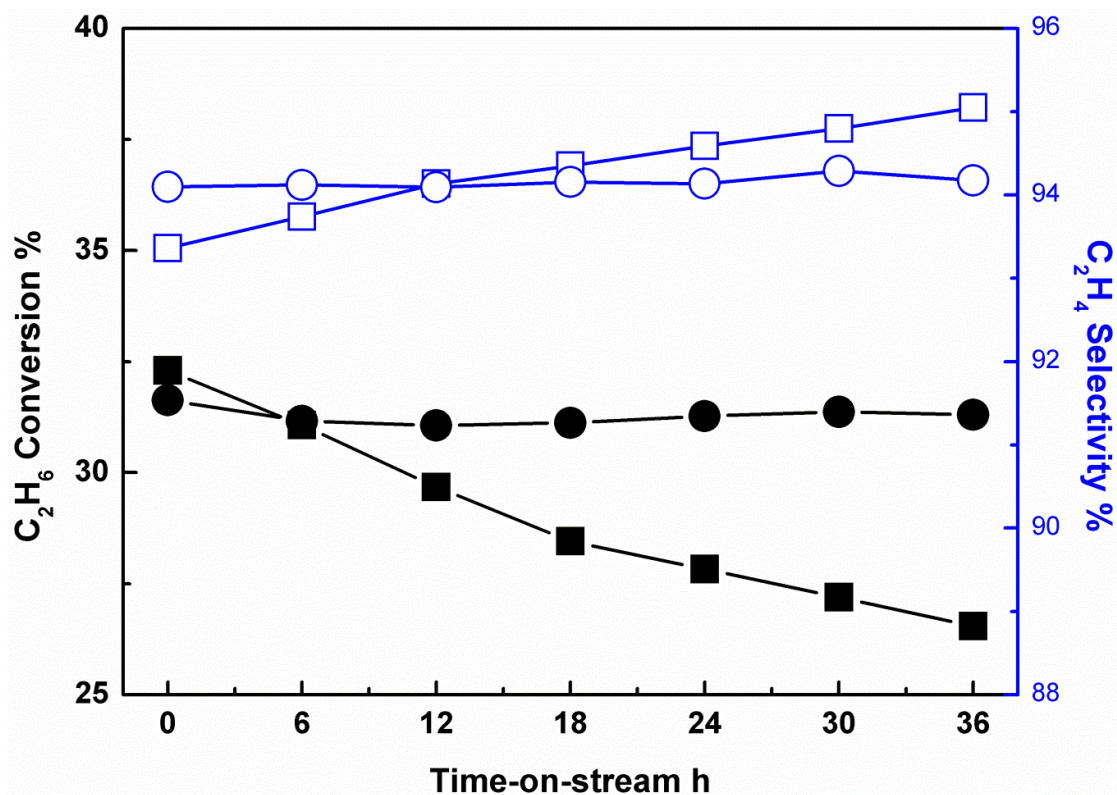


Figure 6 Ethane conversion and ethylene selectivity as functions of time-on-stream for catalyst A and B. Experiments were performed at 420 °C with a contact time of 20.74 $\text{g}_{\text{cat}} \cdot \text{h} / \text{mol}_{\text{C}_2\text{H}_6}$ for Catalyst A and 6.91 $\text{g}_{\text{cat}} \cdot \text{h} / \text{mol}_{\text{C}_2\text{H}_6}$ for Catalyst B and a reactor inlet $\text{C}_2\text{H}_6/\text{O}_2/\text{He}$ molar ratio of 30/20/50

(■) ethane conversion of catalyst A (□) ethylene selectivity of Catalyst A
 (●) ethane conversion of catalyst B (○) ethylene selectivity of Catalyst B

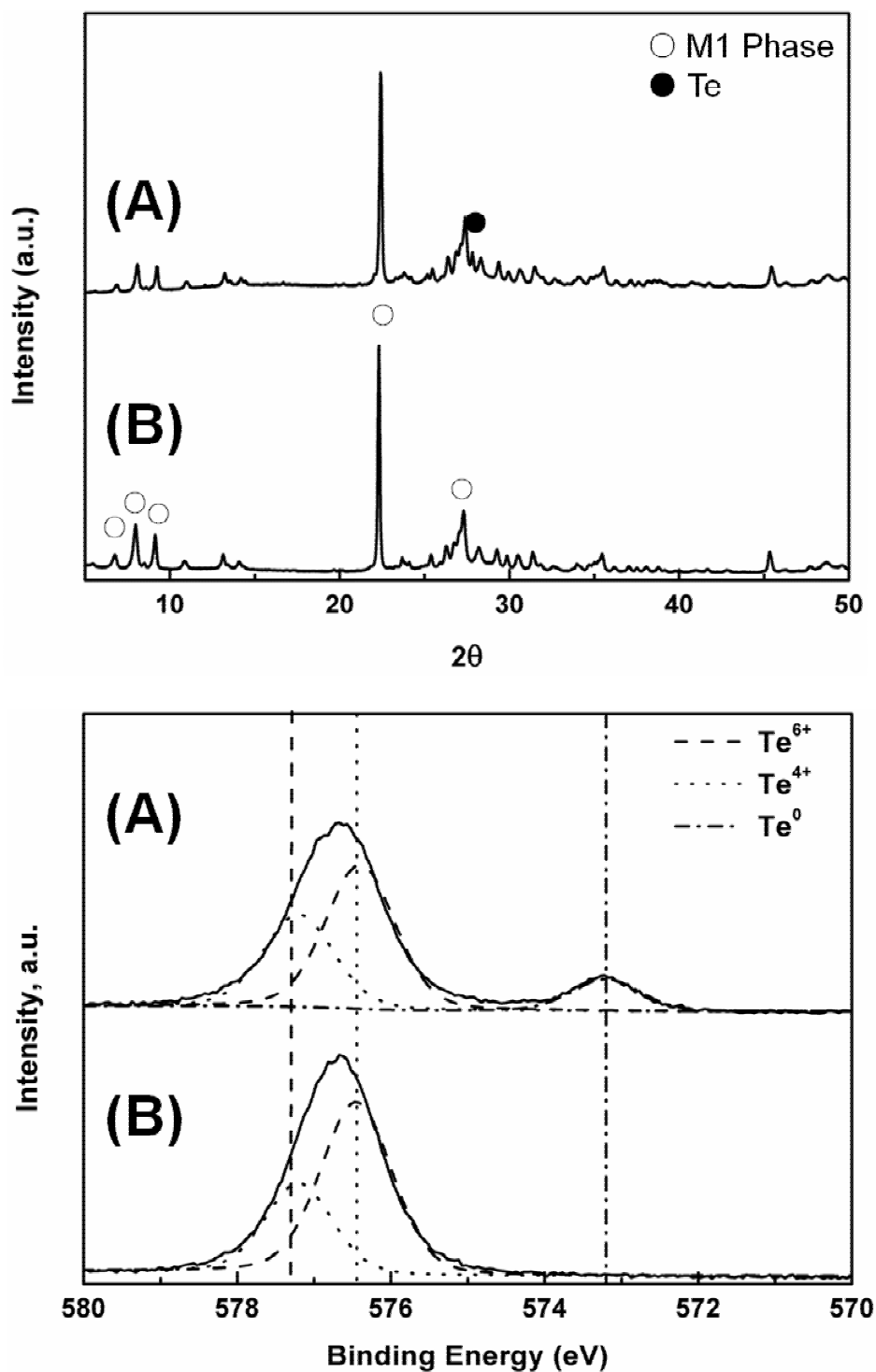


Figure 7 XRD patterns (above) and XPS spectra (below) for used catalyst (A) Catalyst A and (B) Catalyst B

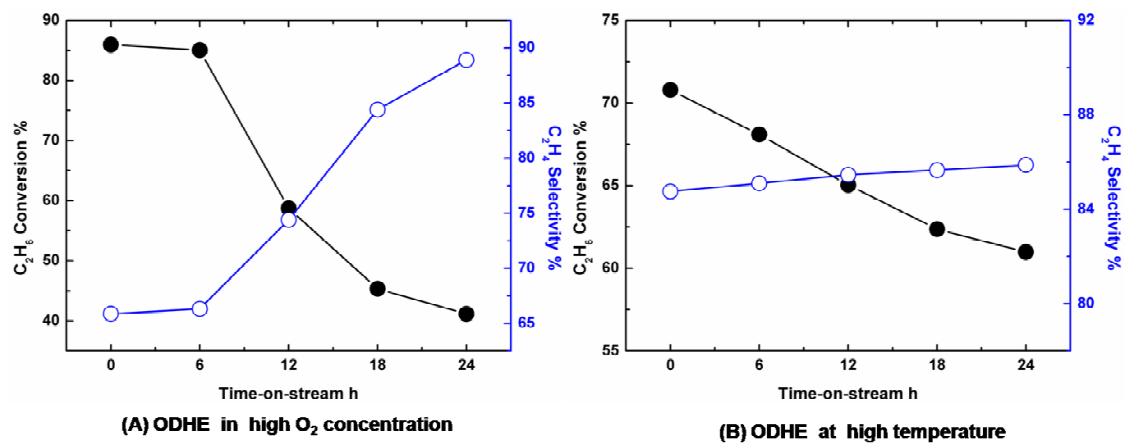


Figure 8 Ethane conversion (●) and ethylene selectivity (○) as functions of time-on-stream for catalyst B under harsh conditions. Experiments were performed at (A) 400 °C with a space time of 20.74 g_{cat}·h/mol_{C₂H₆} and a reactor inlet C₂H₆/O₂/He molar ratio of 30/40/30 and (B) 460 °C with a space time of 20.74 g_{cat}·h/mol_{C₂H₆} and a reactor inlet C₂H₆/O₂/He molar ratio of 30/20/50

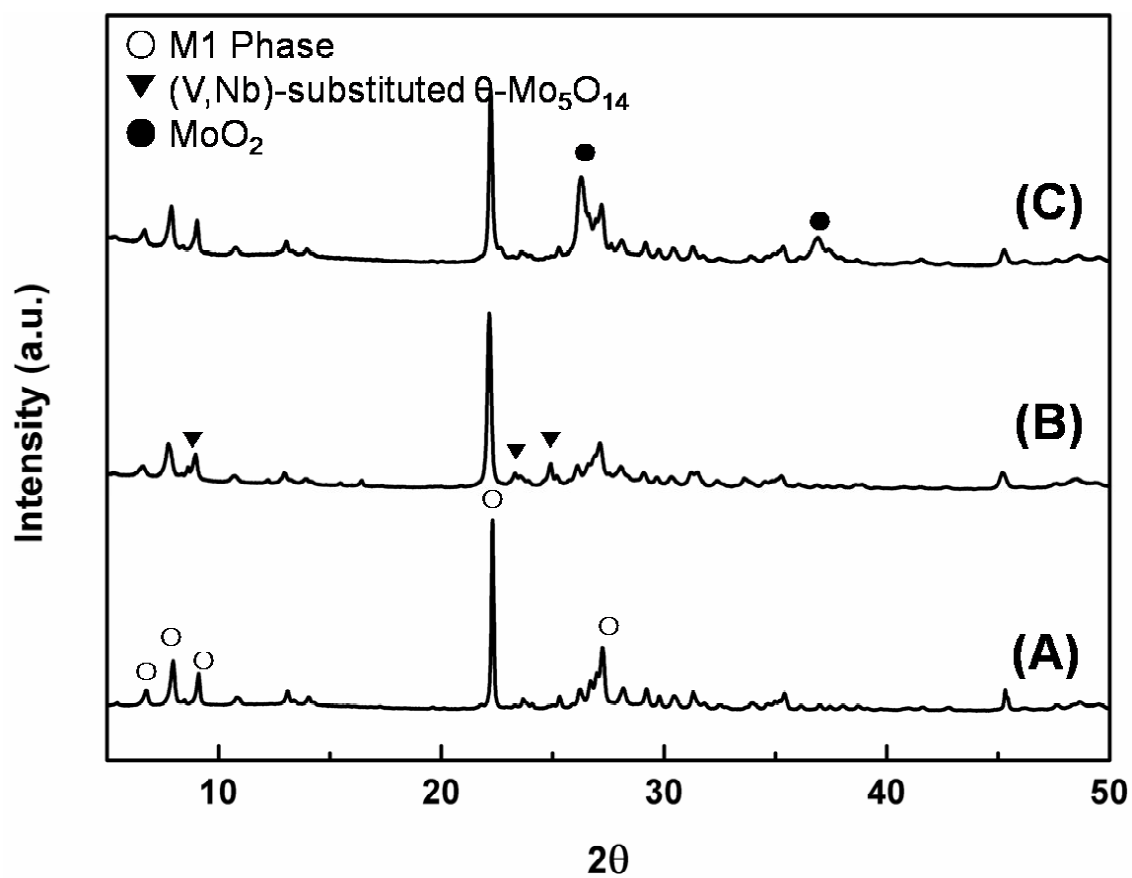


Figure 9 XRD patterns of (A) fresh catalyst B (B) used catalyst B after ODHE in high O_2 concentration and (C) used catalyst B after ODHE at high temperature.

Tables

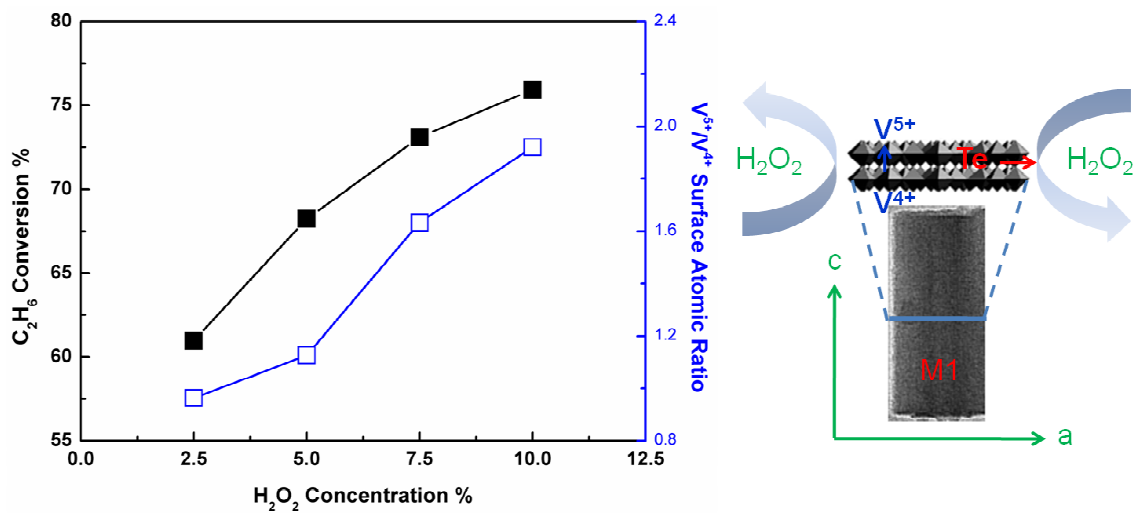
Table 1 General properties of the MoVNbTeO_x catalysts

	Catalyst A	Catalyst B	Catalyst C	Catalyst D
Bulk Composition (ICP)	MoV _{0.21} Te _{0.22} Nb _{0.19}	MoV _{0.19} Te _{0.08} Nb _{0.28}	MoV _{0.20} Te _{0.11} Nb _{0.28}	MoV _{0.16} Te _{0.09} Nb _{0.30}
Surface Composition (XPS)	MoV _{0.13} Te _{0.29} Nb _{0.17}	MoV _{0.13} Te _{0.09} Nb _{0.30}	MoV _{0.15} Te _{0.09} Nb _{0.27}	MoV _{0.11} Te _{0.11} Nb _{0.38}
Particle diameter (TEM) ^a , nm	110.2	106.3	52.1	22.1
Particle diameter (XRD) ^b , nm	>100	>100	49.8	22.6
Surface Area (BET), m ² /g	9.56	17.63	28.14	53.78
Unit cell parameters <i>Pba</i> 2, Å	a = 21.1632 b = 26.6876 c = 4.01532	a = 21.1874 b = 26.6565 c = 4.01472	a = 21.1678 b = 26.6734 c = 4.01230	a = 21.1338 b = 26.6716 c = 4.01030

a. Determined based on the average diameter of at least 100 particles from the TEM images.

b. Determined based on the half band width of peak at 7.7° in XRD patterns to calculate the average crystal size along the [2 0 0] direction by Scherrer equation.

c. Unit cell parameters for M1 phase is a = 21.1337 Å, b = 26.6440 Å, c = 4.01415 Å [39].



ACCEPTED MANUSCRIPT

Highlights

- Post-treatment effect on ODHE performance of phase-pure M1 catalysts was studied.
- H₂O₂ treatment is effective in M1 catalyst activity and stability improvement.
- M1 catalyst activity is mainly affected by V⁵⁺ and partially affected by Te content
- M1 catalyst stability is affected by Te content and reaction conditions

Accepted Manuscript